850 μm OBSERVATIONS OF THE 11 JULY 1991 TOTAL SOLAR ECLIPSE

M. W. EWELL, JR., H. ZIRIN and J. B. JENSEN
Big Bear Solar Observatory, Caltech 264-33, Pasadena, CA 91125, U. S. A.
and
T. S. BASTIAN
National Radio Astronomy Observatory, P. O. Box O, Socorro, NM 87801, U. S. A.

Abstract. We present observations of the 11 July 1991 total solar eclipse made from the Caltech Submillimeter Observatory. The 850 μm limb is extended 3380±140 km above the visible limb, and there is a 10% brightening at the extreme limb. The measured limb height agrees with previous work at shorter and longer wavelengths. The run of limb heights with wavelength is well fit by a single electron density scale height. We argue that there is no need to invoke spicule geometry to explain the observations.

Key words: eclipses – infrared: stars – Sun: chromosphere

1. The Experiment

The beam size of the CSO antenna is too large to make a meaningful measurement of the solar limb profile under normal conditions. However, at second and third contacts of a total eclipse it is possible to measure the brightness of the solar crescent even when it is smaller that the beam. The limb profile is essentially the time derivative of the observed brightness. In principle, the accuracy of such a measurement is limited only by the roughness of the lunar limb. In practice, the imperfect tracking of the CSO antenna precluded simply pointing at the contact locations; it is not possible to untangle brightness changes due to tracking jitter from the measured brightness profile. We decided instead to drive the antenna back and forth across the solar crescent with a 2 second period. The time of maximum signal can then be used to determine the antenna position. A similar method has been employed by Lindsey *et al.* (1983).

To avoid focusing too much near infrared radiation on the secondary and receiver, we covered the antenna with a Griffolyn tent (see Horne *et al.*, 1981, and Clark *et al.*, 1983). We used an SIS tunnel junction receiver tuned to 353 GHz. A description of this device can be found in Ellison *et al.* (1989). At each contact, we obtained 4000 data points at a sampling rate of 50 Hz. The WWV time reference was monitored at the observatory, so the precise time that each data point was obtained is known to one-sixtieth of a second. The expected 850 μm contact time was centered in the 80 second observation. The peak-to-peak amplitude of the antenna motion was 30 arcsec for second contact, and 70 arcsec for third contact.

The raw data for both contacts is shown in Figure 1. The position of the visible limb is also indicated. Several points are immediately apparent. Emission is detected well above the visible limb. The motion of the antenna across the lunar limb is evident when there is no solar signal. The peaks are narrower in the third contact data because the antenna was traversing more quickly, and the alternation between wide and narrow peaks was due to the earth's rotation alternately assisting and

D. M. Rabin et al. (eds.), Infrared Solar Physics, 161–166.

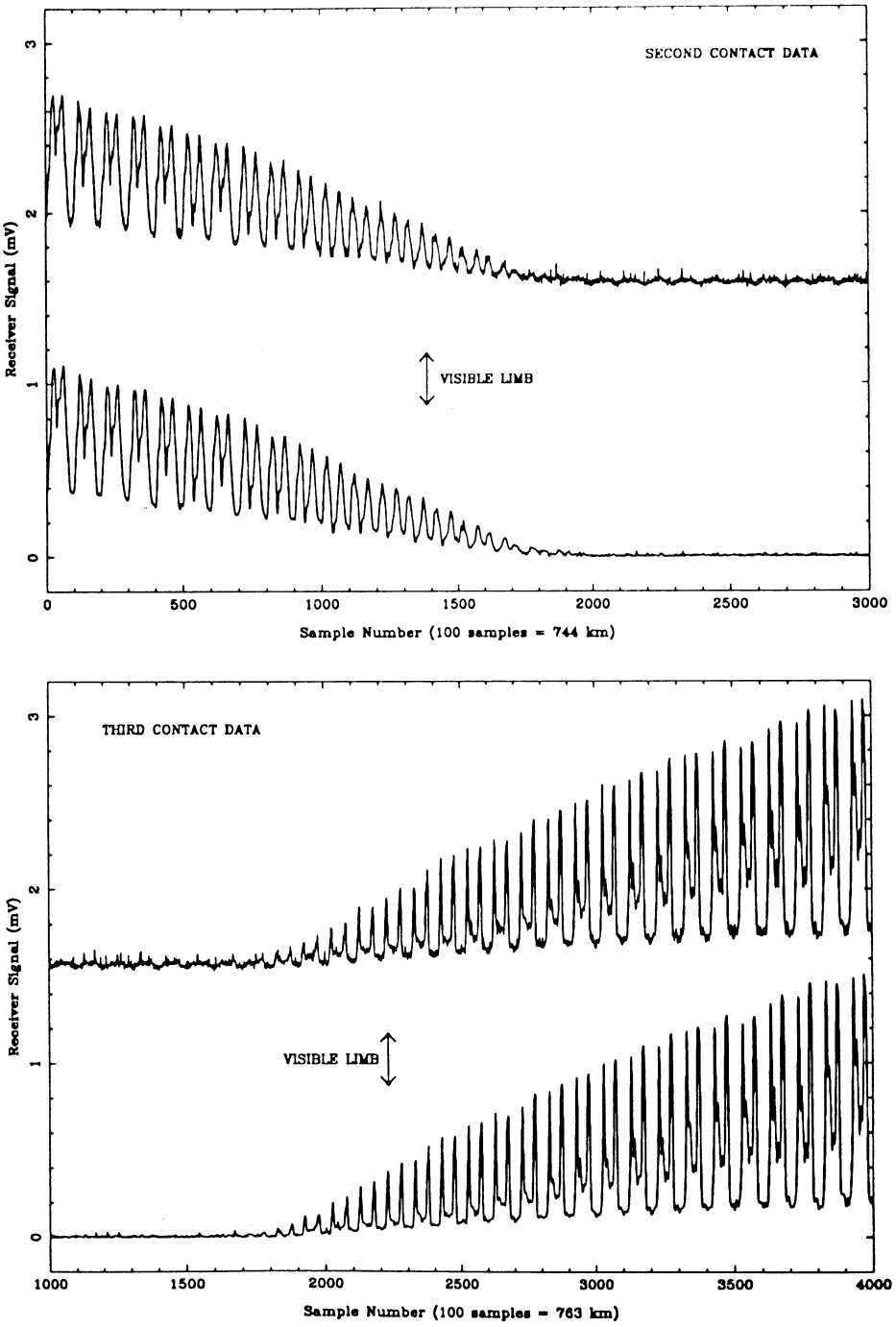

Fig. 1. The raw and smoothed data from second and third contacts.

https://doi.org/10.1017/S0074180900124386 Published online by Cambridge University Press

opposing the telescope motion. The structures between the peaks are due to antenna transients. The heights of the peaks depart from a smooth curve by more than can be accounted for by receiver noise. This effect is due to variations in the atmosphere; the eclipse occured at a 69° zenith angle, and the weather conditions were less than ideal. The sky and moon contributions were subtracted, and the data was then smoothed using a robust non-parametric scheme prescribed by Tukey (1977). The smoothed data is also shown in Figure 1.

The one dimensional beam profile of the CSO antenna was measured by performing a series of drift scans across the lunar limb during the partial phase of the eclipse. The beam profile has also been measured at 290 GHz by Serabyn *et al.* (1991) using shear interferometry. They found that the beam had a 25″ FWHM gaussian core and an 80″ extended plateau (20.6″ and 66″ respectively, when scaled to 353 GHz). Our drift scans were consistent with these values, but we also detected an extended component that was well fit by a 440″ FWHM gaussian containing about 17% of the total power. This three component beam was used in the moon subtraction mentioned above, and also in the limb profile determination described in the next section.

2. The Limb Profile

The limb profile is determined from the heights and positions of the peaks in the data. The solar limb is divided into bins whose widths are given by the time separation of the peaks multiplied by the speed of the lunar limb. Each bin is considered in turn, starting with the outermost. A position for the antenna beam is assumed, the brightness of the bin is adjusted to give the observed signal, the position of the beam is moved to the point which would give the maximum signal, and the procedure is iterated until it converges to consistent values for the beam position and bin brightness. Beam deconvolution and differentiation are thus performed simultaneously and self-consistently. If this method is applied directly to the raw data, several of the bins are assigned a negative brightness. This is because the peak heights are not monotonically increasing due to the atmospheric fluctuations. To get around this difficulty, we first fit a quadratic to the peak heights, and used the fitted values in the subsequent analysis. However, for peaks above the limb, we retained the unfitted values. A more complete description of the data reduction can be found in Ewell *et al.* (1992).

The measured third contact limb is shown in Figure 2. The peak which corresponds to the half-brightness point occured at 17:32:07.8 UT. Visible third contact, with the lunar limb correction applied, occured at 17:32:16.9 UT (Bangert *et al.*, 1989), and the speed of the lunar limb at third contact was 0.50535 arcsec s^{-1}. This gives a 850 μm limb height of 4.6±0.5 arcsec, or 3390±190 km. The error bars are set to one-half of the distance between peaks. The second contact peak at this same brightness level occured at 17:28:18.2 UT, with visible contact at 17:28:09.4 UT and a lunar speed of 0.51843 arcsec s^{-1}, giving a limb height of 3360±190 km. The extremely close agreement between these two values is fortuitous, but it leaves little doubt as to the reliability of the result. Combining the two measurements gives our quoted value of 3380±140 km.

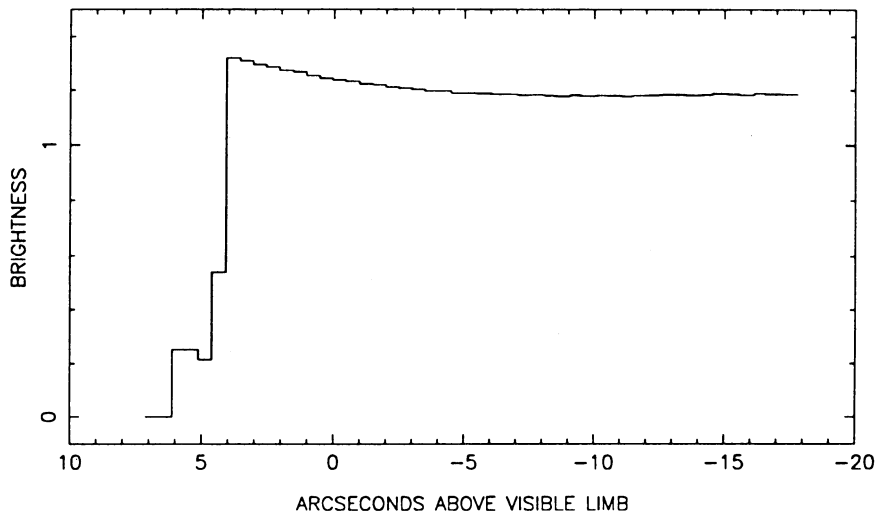

Fig. 2. The third contact limb profile. The half-power point is 4.6″ above the visible limb. The overall normalization is uncertain, but there is clearly a limb brightening of about 10%.

The brightness in Figure 2 is normalized to unit brightness at sun center. There is clearly a 10% brightening in the 5 arcseconds just inside the limb. Of necessity the sun center measurements were taken several minutes before the contact measurements, and because of the atmospheric conditions, the calibration is somewhat uncertain. Therefore, we cannot determine whether the 20% brightening 20 arcseconds inside the limb is real, giving a total limb brightening of 30%, or whether it is simply a calibration error.

3. Discussion

Table 1 shows how our limb height measurement at 850 μm compares with previous measurements by Roellig *et al.* (1991) at 200, 360 and 670 μm and with the value found by Belkora *et al.* (1992) for this eclipse at 3 mm. The data are in mutual agreement, all following a general trend. Table 1 also gives the limb heights predicted by VAL model C (Vernazza *et al.*, 1981), the "standard" model of the solar atmosphere. There is a large and statistically significant discrepency at all listed wavelengths; the far infrared and submillimeter limbs are extended well above where they occur in the VAL. This extension has already been noted by Lindsey *et al.* (1986) as evidence that the chromosphere is not in hydrostatic equilibrium.

We have constructed a very simple model (the Caltech Irreference Chromospheric Model, or CICM) which fits all of the observed limb heights with essentially one adjustable parameter. The opacity source for the conditions and wavelengths of interest is free-free absorption, so we model only temperature and electron density.

https://doi.org/10.1017/S0074180900124386 Published online by Cambridge University Press

TABLE I
Limb Heights, Calculated and Observed

Wavelength (μm)	Observed (km)	VAL limb (km)	CICM limb (km)
200	1450±200	900	1550
360	2300±200	1400	2300
670	3300±200	1700	3100
850	3380±140	1800	3400
3000	5500±400	1800	5400

We use the VAL up to the temperature minimum at 525 km, above which the temperature increases to 6500 K at 1400 km, and to 7500 K at 5000 km. (Model heights are referenced to the photosphere as in the VAL: note that all other heights given in this paper are referenced to the visible limb.) The results are not sensitive to changes of a few hundred kilometers in the 6500 K height; the value adopted is also from the VAL. The temperature at 5000 km was chosen to agree with measurements between 1.4 GHz and 18 GHz by Zirin *et al.* (1991). We take the electron density to fall exponentially from the temperature minimum, and the electron density scale height is our single adjustable parameter. The ionization fraction could be changing rapidly in the modeled region, so the connection between electron density and total density is not clear. The values shown in Table 1 are for a scale height of 1200 km. The agreement with the observations is remarkable; it is not necessary to invoke a rough atmosphere in order to fit the data.

There is an independent line of argument against a rough atmosphere model. Consider the high resolution limb pictures taken at various offsets in the Hα line by R. B. Dunn at Sac Peak (Lynch *et al.*, 1973). The spicules are seen to be sharp and distinct at 0.75 Å and 1 Å from line center, respectively. But at line center, the top of the Hα emission is smooth, and is *higher* than the spicules. Thus it is clear that, at least in Hα, the atmosphere does not have a rough top. Moreover, the height of the Hα limb agrees with the limb height at 3 mm.

Finally, we would like to point out that there is also an independent line of argument showing that the chromosphere is not in hydrostatic equilibrium. Elements with a high first ionization potential are well known to be underabundant in the corona by about a factor of 4 (*c.f.* Breneman and Stone, 1985). The details of the fractionation process are not known, but it clearly involves the acceleration of charged particles. Even if the process was 100% efficient, to achieve the observed abundances it would need to act on 75% of the total mass that reaches the corona, and on an even higher fraction with less than perfect efficiency. Thus most of the mass in the chromosphere is being subjected to accelerations that are not accounted for in the standard atmosphere models, and it is not surprising that the assumption of hydrostatic equilibrium yields predicted limb heights that are unequivocally ruled out by the observations.

Acknowledgements

We would like to thank Prof. Tom Phillips for letting us point his telescope at the sun, Dr. Gordon Hurford for developing the Griffolyn tent, Ms. Michal Peri for help cutting it, Antony Schinckel for his high-altitude acrobatics, and Taco Machilvi for his computer wizardry. We would also like to thank Prof. E. Avrett for several conversations on chromospheric models.

This work was supported by NSF grants AST-9015139, AST-9015755, and by a Caltech SURF.

References

Bangert, J. A., Fiala, A. D., and Harris, W. T.: 1989, *United States Naval Observatory Circular No. 174.*

Belkora, L., Hurford, G. J., Gary, D. E., and Woody, D.: 1992, *Astrophys. J.*, submitted.

Breneman, H. H., and Stone, E. C.: 1985, *Astrophys. J. (Letters)* **299**, L57.

Clark, T. A., Kendall, D. J. W., and Boreiko, R. T.: 1983, *Infrared Phys.* **23**, 289.

Ellison, B. N., Schaffer, P. L., Schaal, W., Vail, D., and Miller, R. E.: 1989, *Int'l J. IR & MM Waves* **10**, 8.

Ewell, M. W., Jr., Zirin, H., Jensen, J. B., and Bastian, T. S.: 1992, *Astrophys. J.*, submitted.

Horne, K., Hurford, G. J., Zirin, H., and de Graauw, Th.: 1981, *Astrophys. J.* **244**, 340.

Lindsey, C., Becklin, E. E., Jefferies, J. T., Orrall, F. Q., Werner, M. W., and Gatley, I.: 1983, *Astrophys. J. (Letters)* **264**, L25.

Lindsey, C., Becklin, E. E., Orrall, F. Q., Werner, M. W., Jefferies, J. T., and Gatley, I.: 1986, *Astrophys. J.* **308**, 448.

Lynch, D. K., Beckers, J. M., and Dunn, R. B.: 1973, *Solar Phys.* **30**, 63.

Roellig, T. L., Becklin, E. E., Jefferies, J. T., Kopp, G. A., Lindsey, C. A., Orrall, F. Q., and Werner, M. W.: 1991, *Astrophys. J.* **381**, 288.

Serabyn, E., Phillips, T. G., and Masson, C. R.: 1991, *Appl. Optics* **30**, 1227.

Tukey, J. W.: 1977, *Exploratory Data Analysis*, Addison-Wesley, Reading, p.523.

Vernazza, J., Avrett, E. H., and Loeser, R.: 1981, *Astrophys. J. Suppl.* **45**, 635.

Zirin, H., Baumert, B. M., and Hurford, G. J.: 1991, *Astrophys. J.* **370**, 779.